An exact collisionless equilibrium for the force-free Harris sheet with low plasma beta

Article

Published Version

O. Allanson, T. Neukirch, F. Wilson, and S. Troscheit

Articles you may be interested in
Force-free Jacobian equilibria for Vlasov-Maxwell plasmas
Phys. Plasmas **20**, 102117 (2013); 10.1063/1.4826502

Plasma-beta dependence of the fast reconnection mechanism in an initially force-free current sheet
Phys. Plasmas **18**, 102903 (2011); 10.1063/1.3655449

A detailed investigation of the properties of a Vlasov–Maxwell equilibrium for the force-free Harris sheet
Phys. Plasmas **16**, 122102 (2009); 10.1063/1.3268771

Computer studies on the spontaneous fast reconnection evolution in a force-free current sheet system
Phys. Plasmas **9**, 816 (2002); 10.1063/1.1447257

Nonlinear gyroviscous force in a collisionless plasma
Phys. Plasmas **8**, 3936 (2001); 10.1063/1.1389093
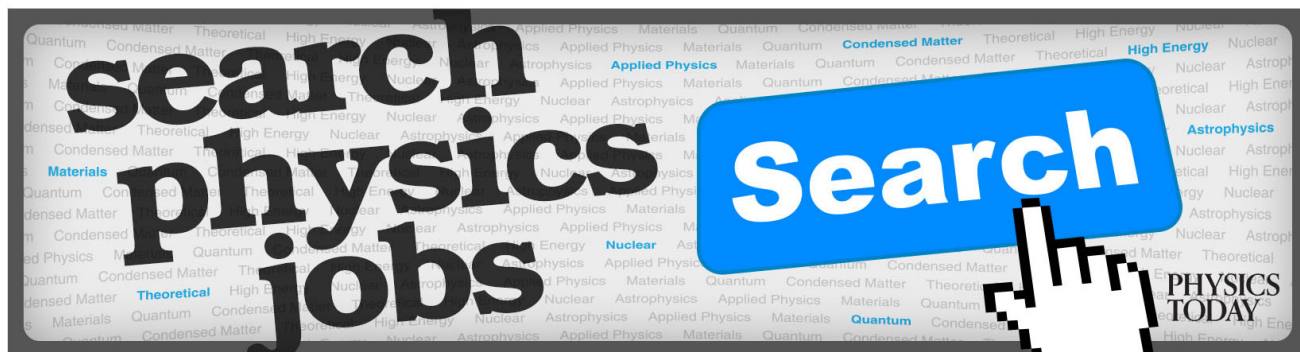
An exact collisionless equilibrium for the Force-Free Harris Sheet with low plasma beta

O. Allanson,[a)] T. Neukirch,[b)] F. Wilson,[c)] and S. Troscheit[d)]
School of Mathematics and Statistics, University of St Andrews, St. Andrews, KY16 9SS, United Kingdom

We present a first discussion and analysis of the physical properties of a new exact collisionless equilibrium for a one-dimensional nonlinear force-free magnetic field, namely, the force-free Harris sheet. The solution allows any value of the plasma beta, and crucially below unity, which previous nonlinear force-free collisionless equilibria could not. The distribution function involves infinite series of Hermite polynomials in the canonical momenta, of which the important mathematical properties of convergence and non-negativity have recently been proven. Plots of the distribution function are presented for the plasma beta modestly below unity, and we compare the shape of the distribution function in two of the velocity directions to a Maxwellian distribution. © 2015 Author(s). All article content, except where otherwise noted, is licensed under a Creative Commons Attribution 3.0 Unported License.
[http://dx.doi.org/10.1063/1.4934611]

I. INTRODUCTION

Equilibria are a suitable starting point for investigations of plasma instabilities and waves. Force-free equilibria, with fields defined by

$$\nabla \cdot \mathbf{B} = 0,$$
$$\nabla \times \mathbf{B} = \mu_0 \mathbf{j}, \qquad (1)$$
$$\mathbf{j} \times \mathbf{B} = 0,$$

are, for example, of particular relevance to the solar corona and other astrophysical plasmas, as well as the scrape-off layer in tokamaks; see, for example, Refs. 1–3, respectively. Equation (1) implies that the current density is everywhere-parallel to the magnetic field

$$\mu_0 \mathbf{j} = \alpha(\mathbf{r})\mathbf{B}, \qquad (2)$$

or zero in the case of potential fields. If $\nabla \alpha \neq 0$ then the force-free field is nonlinear, whereas a constant α corresponds to a linear force-free field. Extensive discussions of force-free fields are given in Refs. 2 and 4.

We consider one-dimensional (1D), non-relativistic collisionless plasmas, for which it is necessary to use kinetic theory. An equilibrium, characterised by the one-particle distribution function (DF), is a solution of the steady-state Vlasov equation.[5] For a macroscopic equilibrium to be described, the DF must solve Maxwell's equations and describe force balance, via the coupling to the charge and current densities, as well as to the pressure. The difficulty of the problem in general lies in achieving self-consistency between the microscopic and macroscopic descriptions.

Current sheets are extremely important for reconnection studies, see Ref. 6, for example. Three families of exact nonlinear force-free Vlasov-Maxwell (VM) equilibria are known,[7–10] all of which describe 1D current sheets. The first family uses the force-free Harris sheet (FFHS) as their magnetic field profile.[7,8] The FFHS magnetic field is given by

$$\mathbf{B} = B_0(\tanh(z/L), \operatorname{sech}(z/L), 0), \qquad (3)$$

with L being the width of the current sheet, and B_0 being the constant magnitude of the magnetic field. The second example uses Jacobi elliptic functions, of which the FFHS is a special case.[9] The third example[10] will be discussed herein. We note work on "nearly" force-free equilibria,[11] with the FFHS modified by adding a small B_z component. Examples of linear force-free VM equilibria[12–17] are discussed in Ref. 18.

Two of the nonlinear force-free DFs known thus far[7–9] have the "drawback" of describing plasmas with a plasma-beta (β_{pl}) greater than one, due to the manner in which they were constructed. β_{pl} is defined as the ratio of the thermal energy density to the magnetic energy density

$$\beta_{pl} = \sum_s \beta_{pl,s} = \frac{2\mu_0 k_B}{B_0^2} \sum_s n_s T_s, \qquad (4)$$

for n_s and T_s the number density and temperature—of species s—respectively. In Cartesian geometry, and when gravity and electric fields are neglected, the fluid equation of motion[5] becomes

$$\frac{\partial}{\partial x_j} P_{ij} = (\mathbf{j} \times \mathbf{B})_i, \qquad (5)$$

for P_{ij}, the pressure tensor, and the Einstein summation convention applied over repeated indices. In this case, a β_{pl}

a)Electronic mail: oliver.allanson@st-andrews.ac.uk
b)Electronic mail: tn3@st-andrews.ac.uk
c)Electronic mail: fw237@st-andrews.ac.uk
d)Electronic mail: s.troscheit@st-andrews.ac.uk

much less than one is typically taken to be consistent with a force-free magnetic field. In the case of one "dynamical" component of the pressure tensor, P, force balance is described by $\nabla P = \mathbf{j} \times \mathbf{B}$ and $\beta_{pl} = 2\mu_0 P / B_0^2$.

The basic theory of the technique used to reach the low plasma-beta regime, and the posing of the inverse problem are explained in Section II. Section III explains the inversion procedure used to find an equilibrium solution, with full detail in Ref. 10. In Section IV, we present a discussion of some of the properties of the distribution function in the numerically accessible parameter regime. The first order moments of the DF are calculated in the Appendixes, and used in Section IV to calculate the current sheet width. Finally, we close with a summary and conclusions.

II. BASIC THEORY

An exact solution of the Vlasov equation is necessarily a function of the constants of motion.[5] The equilibrium we shall consider varies only in one Cartesian spatial coordinate, namely, z. This implies that the Hamiltonian, H_s, and the x and y canonical momenta, p_{xs} and p_{ys} for each particle species

$$H_s = m_s v^2 / 2 + q_s \phi,$$
$$p_{xs} = m_s v_x + q_s A_x,$$
$$p_{ys} = m_s v_y + q_s A_y,$$

are conserved, with q_s being the charge of species s and ϕ being the scalar potential. A_x and A_y are components of the vector potential, with $A_z = 0$ and $\mathbf{B} = \nabla \times \mathbf{A}$. The Vlasov equation can now be solved by any differentiable function $f_s(H_s, p_{xs}, p_{ys})$, with the additional "physical" constraints being that f_s is also normalisable, non-negative and has velocity moments of arbitrary order.[5] The assumption of quasineutrality, $\sigma(z) = 0$, implicitly defines the scalar potential as a function of the vector potential, $\phi_{qn}(A_x, A_y)$.[18] For DFs of the form considered in this paper, see equation (11), the quasineutral scalar potential takes the form

$$\phi_{qn}(A_x, A_y) = \frac{1}{e(\beta_e + \beta_i)} \ln(n_i / n_e). \tag{6}$$

To be able to use the method of Channell[12] (described later), we choose our parameters such that strict neutrality ($n_i(A_x, A_y) = n_e(A_x, A_y)$) is satisfied. As already pointed out in Ref. 18, this implies that $\phi_{qn} = 0$ due to Equation (6). Our choice of parameters is mathematically equivalent to the condition used to derive micro-macroscopic parameter relationships, which will be discussed in Section III.

It has been shown in Refs. 18–23, for example, that the 1D Vlasov-Maxwell equilibrium problem is analogous to that of a particle moving under the influence of a potential; with the relevant component of the pressure tensor, P_{zz}, taking the role of the potential; (A_x, A_y) the role of position and z the role of time. Under our assumptions this means that

$$\frac{d^2 A_x}{dz^2} = -\mu_0 \frac{\partial P_{zz}}{\partial A_x}, \tag{7}$$

$$\frac{d^2 A_y}{dz^2} = -\mu_0 \frac{\partial P_{zz}}{\partial A_y}. \tag{8}$$

These equations (or equivalent) are first seen in a complete sense in Ref. 24. Furthermore, the force-free equilibrium fields correspond to a *trajectory*, $(A_x(z), A_y(z))$, that is itself a *contour*

$$\frac{dP_{zz}}{dz} = 0, \tag{9}$$

of the *potential*, P_{zz}.[7] Equations (7)–(9) succinctly define the problem of calculating a 1D, quasineutral, force-free equilibrium. The difficulty lies in calculating the DF, f_s, given a macroscopic expression for $P_{zz}(A_x, A_y)$, formally defined

$$P_{zz} = \sum_s P_{zz,s} = \sum_s m_s \int w_z^2 f_s d^3 v, \tag{10}$$

for $w_z = v_z - \langle v_z \rangle_s$, with v_z, the particle velocity and $\langle v_z \rangle_s$, the bulk velocity of species s in the z direction. Channell developed the theory of this problem,[12] with the added assumption of zero scalar potential from the offset, and a distribution function of the form

$$f_s = \frac{n_{0s}}{\left(\sqrt{2\pi} v_{th,s}\right)^3} e^{-\beta_s H_s} g_s(p_{xs}, p_{ys}). \tag{11}$$

The species dependent constants are n_{0s}, thermal velocity $v_{th,s}$ and $\beta_s = 1/(k_B T_s)$. The "perturbation" to the Maxwellian, g_s, is an as yet unknown function of the canonical momenta. Note that the DF defined in Equation (11) is an even function of v_z, giving no bulk flow in the z direction, and hence $\langle v_z \rangle_s = 0$. After integrating over v_z, the assumption of Equation (11) in Equation (10) leads to

$$
\begin{aligned}
P_{zz}(A_x, A_y) = {} & \frac{\beta_e + \beta_i}{\beta_e \beta_i} \frac{n_{0s}}{2\pi m_s^2 v_{th,s}^2} \\
& \times \int_{-\infty}^{\infty} \int_{-\infty}^{\infty} e^{-\beta_s \left((p_{xs} - q_s A_x)^2 + (p_{ys} - q_s A_y)^2\right) / (2m_s)} \\
& \times g_s(p_{xs}, p_{ys}) dp_{xs} dp_{ys}.
\end{aligned}
\tag{12}
$$

Equation (12) defines mathematically the inverse problem at hand: given a known macroscopic equilibrium, characterised by $P_{zz}(A_x, A_y)$, can we invert the integral equation to solve for $g_s(p_{xs}, p_{ys})$?

The inverse problem is not only non-unique regarding the form of the distribution function for a particular macroscopic equilibrium, but also for the form of $P_{zz}(A_x, A_y)$ for a given magnetic field. Given a specific magnetic field, i.e., a specific (A_x, A_y), and a known P_{zz} that satisfies Equations (7)–(9), one can construct infinitely many new $\bar{P}_{zz}$ that also satisfy them

$$\bar{P}_{zz} = \psi'(P_{ff})^{-1} \psi(P_{zz}), \tag{13}$$

for differentiable and non-constant ψ, provided the LHS is positive (see Ref. 18 for a discussion). These $\bar{P}_{zz}$ maintain a force-free equilibrium with the *same magnetic field* as P_{zz}. The value of P_{zz} evaluated on the force-free contour is P_{ff}. This paper takes the P_{zz} used in Refs. 7, 8, and 25 and transforms it as in Equation (13) with the exponential function according to

$$\psi(P_{zz}) = \exp\left[\frac{1}{P_0}(P_{zz} - P_{ff})\right], \qquad (14)$$

with P_0 a free, positive constant. This gives $\bar{P}_{zz,ff} = P_0$, and so the plasma pressure can be as low or high as desired. Channell showed[12] that under the assumptions used in this paper

$$P_{zz}(A_x, A_y) = \frac{\beta_e + \beta_i}{\beta_e \beta_i} n(A_x, A_y), \qquad (15)$$

where $n = n_i = n_e$. Equation (4) then gives

$$\beta_{pl} = \frac{2\mu_0 P_{zz,ff}}{B_0^2} = \frac{2\mu_0 P_0}{B_0^2}.$$

Hence, a freely chosen P_0 corresponds directly to a freely chosen β_{pl}.

We note here that this pressure transformation can also be implicitly seen for the different linear force-free cases presented in the literature,[12,16,22,23] although this connection has never been made. The pressure function in Ref. 22 (and implicitly in Ref. 16) is an exponentiated version of that in Refs. 12 and 23. A further interesting aspect is that the momentum dependent parts of the distribution functions are also related to each other exponentially.

III. CALCULATING THE DISTRIBUTION FUNCTION

The Harrison-Neukirch pressure function[7] is given by

$$P_{zz} = \frac{B_0^2}{2\mu_0}\left[\frac{1}{2}\cos\left(\frac{2A_x}{B_0 L}\right) + \exp\left(\frac{2A_y}{B_0 L}\right) + b\right], \qquad (16)$$

with $b > 1/2$ contributing to a "background" pressure sourced by a Maxwellian distribution, required for positivity. This is the pressure function that describes $\beta_{pl} > 1$ regimes, and we are to transform according to Equations (13) and (14) in order to realise $\beta_{pl} < 1$, resulting in

$$\bar{P}_{zz} = P_0 \exp\left\{\frac{1}{2\beta_{pl}}\left[\cos\left(\frac{2A_x}{B_0 L}\right) + 2\exp\left(\frac{2A_y}{B_0 L}\right) - 1\right]\right\}.$$

The $-1/(2\beta_{pl})$ term comes from results in Ref. 7 regarding the $b > 1/2$ term and the fact that $P_{ff} = B_0^2/(2\mu_0)$ $(1 + (b - 1/2))$, readily seen for $z = 0$, for example. Note that P_{zz} is constant over z, and so we can evaluate at any z to calculate P_{ff}. Exponentiation of P_{zz} has clearly resulted in a complicated LHS of Equation (12), and so the inverse problem defined above is mathematically challenging.

Since exponentiation of the "summative" pressure function results in a "multiplicative" one, we shall exploit separation of variables by assuming $g_s \propto g_{1s}(p_{xs})g_{2s}(p_{ys})$, whilst noting that $\bar{P}_{zz} \propto \bar{P}_1(A_x)\bar{P}_2(A_y)$. This assumption leads to integral equations of the form

$$\bar{P}_1(A_x) \propto \int_{-\infty}^{\infty} e^{-\beta_s(p_{xs} - q_s A_x)^2/(2m_s)} g_1(p_{xs})dp_{xs}, \qquad (17)$$

$$\bar{P}_2(A_y) \propto \int_{-\infty}^{\infty} e^{-\beta_s(p_{ys} - q_s A_y)^2/(2m_s)} g_2(p_{ys})dp_{ys}, \qquad (18)$$

in which the LHS are formed of exponentiated cosine and exponential functions, respectively. These equations are 1D integral transforms, known primarily as Weierstrass transforms[26]

$$\mathcal{W}[f](x) = \frac{1}{\sqrt{4\pi}}\int_{-\infty}^{\infty} e^{-(x-y)^2/4}f(y)dy, \qquad (19)$$

used as Green's function solutions of the diffusion equation, see Ref. 27, for example. One method of inversion[28] involves the use of Hermite polynomials

$$H_n(x) = (-1)^n e^{x^2}\frac{d}{dx}e^{-x^2},$$

a complete orthogonal set for $f \in L^2(\mathbb{R}, e^{-x^2}dx)$.[29] If one can expand the LHS of Equation (19) in a Maclaurin series (with coefficients of expansion a_n) then the unknown function $f(y)$ can be written as

$$f(y) = \sum_{n=0}^{\infty} a_n H_n(y/2).$$

This is the method that we use to invert Equations (17) and (18), to solve for $g_1(p_{1s})$ and $g_2(p_{ys})$.

In Ref. 10, this inversion procedure was performed, and we shall only outline the approach here. The first step is to Maclaurin expand the exponentiated pressure function of Equation (16) according to Equations (13) and (14). Exponentiation of a power series is a combinatoric problem and was tackled by Bell in Ref. 30. If $h(x) = \exp k(x)$ and

$$k(x) = \sum_{n=1}^{\infty} \frac{1}{n!}\zeta_n x^n,$$

then

$$h(x) = \sum_{n=0}^{\infty} \frac{1}{n!}Y_n(\zeta_1, \zeta_2, \ldots, \zeta_n)x^n,$$

for Y_n the nth Complete Bell Polynomial (CBP), and $Y_0 = 1$. These can be defined explicitly for $n \geq 1$ by Faà di Bruno's determinant formula[31] as the determinant of an $n \times n$ matrix

$$Y_n(\zeta_1, \zeta_2, \ldots \zeta_n) = \begin{vmatrix} \binom{n-1}{0}\zeta_1 & \binom{n-1}{1}\zeta_2 & \binom{n-1}{2}\zeta_3 & \cdots & \binom{n-1}{n-2}\zeta_{n-1} & \binom{n-1}{n-1}\zeta_n \\ -1 & \binom{n-2}{0}\zeta_1 & \binom{n-2}{1}\zeta_2 & \cdots & \binom{n-2}{n-3}\zeta_{n-2} & \binom{n-2}{n-2}\zeta_{n-1} \\ 0 & -1 & \binom{n-3}{0}\zeta_1 & \cdots & \binom{n-3}{n-4}\zeta_{n-3} & \binom{n-3}{n-3}\zeta_{n-2} \\ \vdots & \vdots & \vdots & & \vdots & \vdots \\ 0 & 0 & 0 & \cdots & \binom{1}{0}\zeta_1 & \binom{1}{1}\zeta_2 \\ 0 & 0 & 0 & \cdots & -1 & \binom{0}{0}\zeta_1 \end{vmatrix}. \tag{20}$$

For example, $Y_1(\zeta_1) = \zeta_1$ and $Y_2(\zeta_1, \zeta_2) = \zeta_1^2 + \zeta_2$. We include this determinant form here since this is the representation we use to plot the distribution function. Using these results and a simple scaling argument in Ref. 30, the Maclaurin expansion of the transformed pressure is found to be

$$\bar{P}_{zz} = P_0 e^{-1/(2\beta_{pl})} \sum_{m=0}^{\infty} a_{2m} \left(\frac{A_x}{B_0 L}\right)^{2m} \sum_{n=0}^{\infty} b_n \left(\frac{A_y}{B_0 L}\right)^n, \tag{21}$$

with

$$a_{2m} = e^{1/(2\beta_{pl})} \frac{(-1)^m 2^{2m}}{(2m)!} Y_{2m}\left(0, \frac{1}{2\beta_{pl}}, 0, \ldots, 0, \frac{1}{2\beta_{pl}}\right), \tag{22}$$

and

$$b_n = e^{1/\beta_{pl}} \frac{2^n}{n!} Y_n\left(\frac{1}{\beta_{pl}}, \ldots, \frac{1}{\beta_{pl}}\right). \tag{23}$$

This allows us to formally solve the inverse problem for the unknown functions $g_{1s}(p_{xs})$ and $g_{2s}(p_{ys})$ in terms of Hermite polynomials, giving

$$f_s(H_s, p_{xs}, p_{ys}) = \frac{n_{0s}}{\left(\sqrt{2\pi} v_{th,s}\right)^3} \left[e^{-1/(2\beta_{pl})} \sum_{m=0}^{\infty} C_{2m,s} H_{2m} \right.$$
$$\left. \times \left(\frac{p_{xs}}{\sqrt{2} m_s v_{th,s}}\right) \sum_{n=0}^{\infty} D_{ns} H_n \left(\frac{p_{ys}}{\sqrt{2} m_s v_{th,s}}\right) \right] e^{-\beta_s H_s}, \tag{24}$$

for species-dependent and as yet unknown coefficients $C_{2m,s}$ and D_{ns}. The reason for this ambiguity is that the transforms defining our problem in Equations (17) and (18) are not quite of the perfect form of the Weierstrass transform in Equation (19). Since P_{zz} is independent of species—see Equation (21)—we have to ensure that taking the second moment of f_i gives the same result as that of f_e, i.e., when computing the integral of Equation (12). This is solved by fixing the parameters according to

$$n_{0i} = n_{0e} = n_0, \quad P_0 = n_0 \frac{\beta_e + \beta_i}{\beta_e \beta_i}$$

$$C_{2m,s} = \left(\frac{\delta_s}{\sqrt{2}}\right)^{2m} a_{2m}, \quad D_{ns} = \text{sgn}(q_s)^n \left(\frac{\delta_s}{\sqrt{2}}\right)^n b_n.$$

The dimensionless parameter $\delta_s > 0$ is the species-dependent *magnetisation parameter*,[32] also used as the fundamental ordering parameter in gyrokinetics[33]

$$\delta_s = \frac{m_s v_{th,s}}{|q_s| B_0 L} \Rightarrow \frac{\delta_e}{\delta_i} = \sqrt{\frac{m_e T_e}{m_i T_i}}. \tag{25}$$

It is the ratio of the thermal Larmor radius of species s, $\rho_s = v_{th,s}/\Omega_s$, for $\Omega_s = q_s B_0/m_s$, to the characteristic length scale of the system, L. When $\delta_s \ll 1$ then particle species s is highly magnetised.

As yet, the distribution of Equation (24), together with the micro-macroscopic conditions, is only a formal solution to the inverse problem posed. To be valid, it must be convergent, bounded, and non-negative. We note here that infinite series in Hermite polynomials in velocity were used in Vlasov equilibrium studies in Refs. 34 and 35, with the particular question of convergence raised in Ref. 34. Convergence of our infinite series, as well as non-negativity and boundedness properties are proven in Ref. 10, and so will not be repeated here.

IV. PROPERTIES OF THE DISTRIBUTION FUNCTION

The nature of the inverse problem is to calculate a microscopic description of a system, given certain prescribed macroscopic data. Hence, one of the main tasks is to find the relationships between the characteristic parameters of each level of description. That is to say, given (B_0, P_0, L), for example, what is their relation to $(m_s, q_s, v_{th,s}, n_{0s})$?

A. Current sheet width

Currently, there are six free parameters that will determine the nature of the equilibrium. These are n_0, β_{pl}, $\beta_{th,i}$, $\beta_{th,e}$, δ_i, and δ_e. n_0 is in principle fixed by ensuring that the DF is normalised to the total particle number. As yet we have no information regarding the width of the current sheet L. To this end, we shall consider bulk velocities $\langle v_x \rangle_s$ and

$\langle v_y \rangle_s$, obtained from the first moment of the DF. The calculations in Appendixes A and B, together with the fact that $B_0 = \sqrt{2\mu_0 P_0 / \beta_{pl}}$ give

$$\langle v_x \rangle_s = \sqrt{\frac{2}{\mu_0 \beta_{pl} P_0}} \frac{1}{L q_s \beta_s} \frac{\sinh\left(\frac{z}{L}\right)}{\cosh^2\left(\frac{z}{L}\right)},$$

$$\langle v_y \rangle_s = \sqrt{\frac{2}{\mu_0 \beta_{pl} P_0}} \frac{1}{L q_s \beta_s} \frac{1}{\cosh^2\left(\frac{z}{L}\right)}.$$

We can identify the coefficient of the z dependent profiles as the amplitude of the bulk velocities, $\langle v_x \rangle_s$ and $\langle v_y \rangle_s$, as u_s, given by

$$u_s = \sqrt{\frac{2}{\mu_0 \beta_{pl} P_0}} \frac{1}{L q_s \beta_s}, \tag{26}$$

giving

$$(u_i - u_e)^2 = \frac{2}{\mu_0 \beta_{pl} P_0 L^2 q^2} \left(\frac{\beta_e + \beta_i}{\beta_e \beta_i}\right)^2, \tag{27}$$

$$\Rightarrow L = \frac{1}{q} \sqrt{\frac{2(\beta_e + \beta_i)}{\mu_0 n_0 \beta_e \beta_i (u_i - u_e)^2 \beta_{pl}}}, \tag{28}$$

where $q = |q_s|$. Interestingly, this is almost identical to the expression found in Ref. 25 for the current sheet width of the Harrison-Neukirch equilibrium, with the addition of the $\beta_{pl}^{1/2}$ factor in the denominator. It is readily seen that, given some fixed B_0, $L \propto \beta_{pl}^{-1/2}$. This makes sense in that, by raising the number density n_0, and hence β_{pl}, there are simply more current carriers available to produce **j**, and hence the width L can reduce. By manipulating Equation (26), one can show that the amplitudes of the fluid velocities are given by

$$\frac{u_s}{v_{th,s}} = 2\text{sgn}(q_s) \frac{\delta_s}{\beta_{pl}} = 2\text{sgn}(q_s) \frac{\rho_s}{L \beta_{pl}}. \tag{29}$$

Once again, this is almost identical to the expression found in Ref. 25, with the addition of a β_{pl} factor in the denominator.

B. Plots of the distribution function

Having found mathematical expressions for the DFs, we now present different plots of their dependence on v_x and v_y, for $z/L = 0, -1, 1$. Plotting f_s is a challenging numerical task, particularly for the low-β_{pl} regime as when $\beta_{pl} < 1/2$, the $C_{2m,s}$ are readily seen to be of the order

$$\left(\frac{1}{\sqrt{2}}\right)^{2m} \frac{(-1)^m}{(2m)!} \left(\frac{\delta_s}{\beta_{pl}}\right)^{2m},$$

since Y_{2m} is a polynomial of order $2m$ in $1/(2\beta_{pl})$. While it has been proven that the series' with which we represent the DFs are convergent for all values of the relevant parameters,
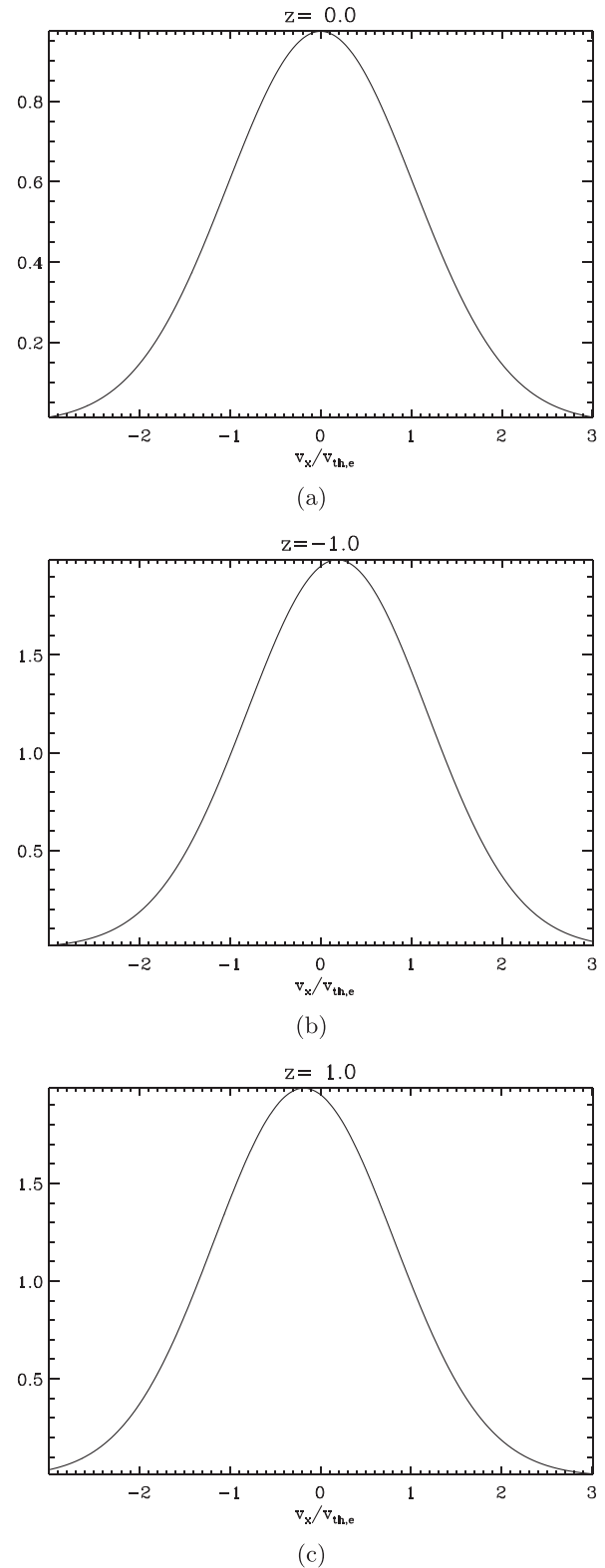

FIG. 1. The v_x variation of f_e for $z/L = 0$ (a), $z/L = -1$ (b), and $z/L = 1$ (c). $\beta_{pl} = 0.85$ and $\delta_e = 0.15$. Note the antisymmetry of the $z = \pm 1$ plots with respect to each other.

attaining numerical convergence for the low-β_{pl} regime, particularly for the p_{xs} dependent sum is thus far proving difficult. Here we present plots for $\beta_{pl} = 0.85$ and $\delta_i = \delta_e = 0.15$. As aforementioned we use Faà di Bruno's determinant formula in Equation (20) to calculate the CBP's, and a
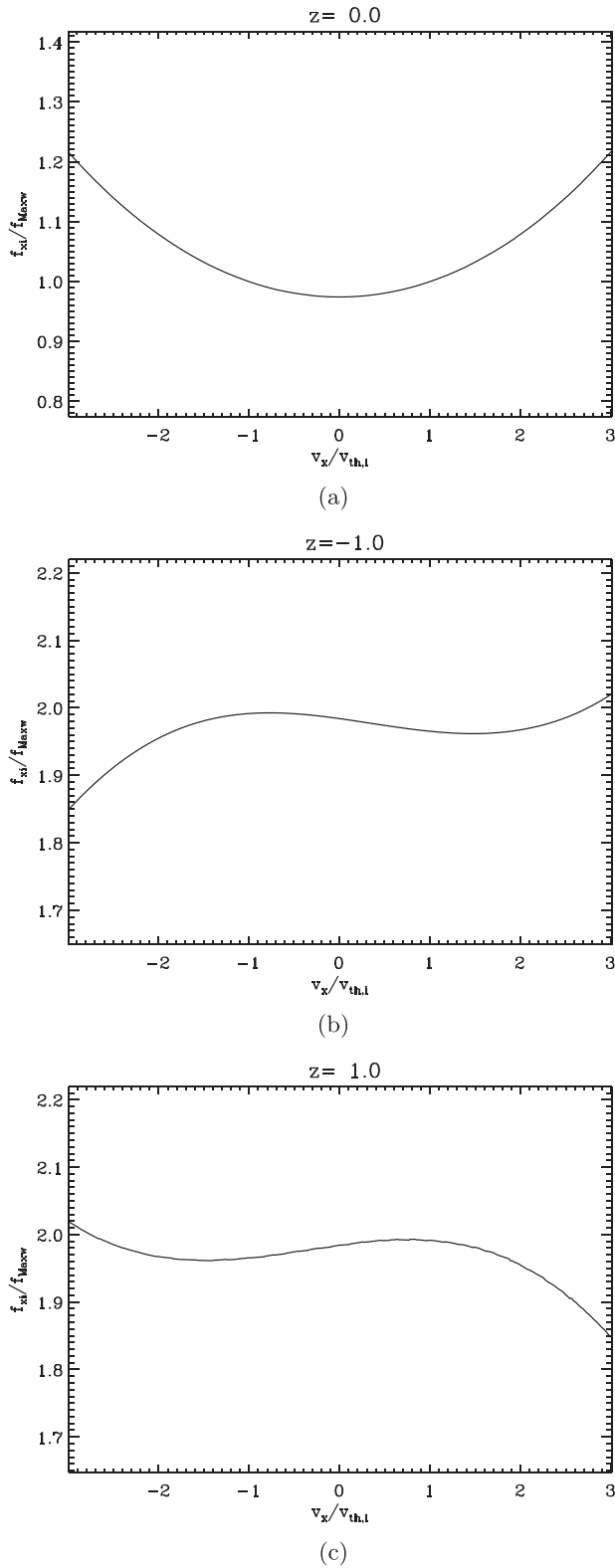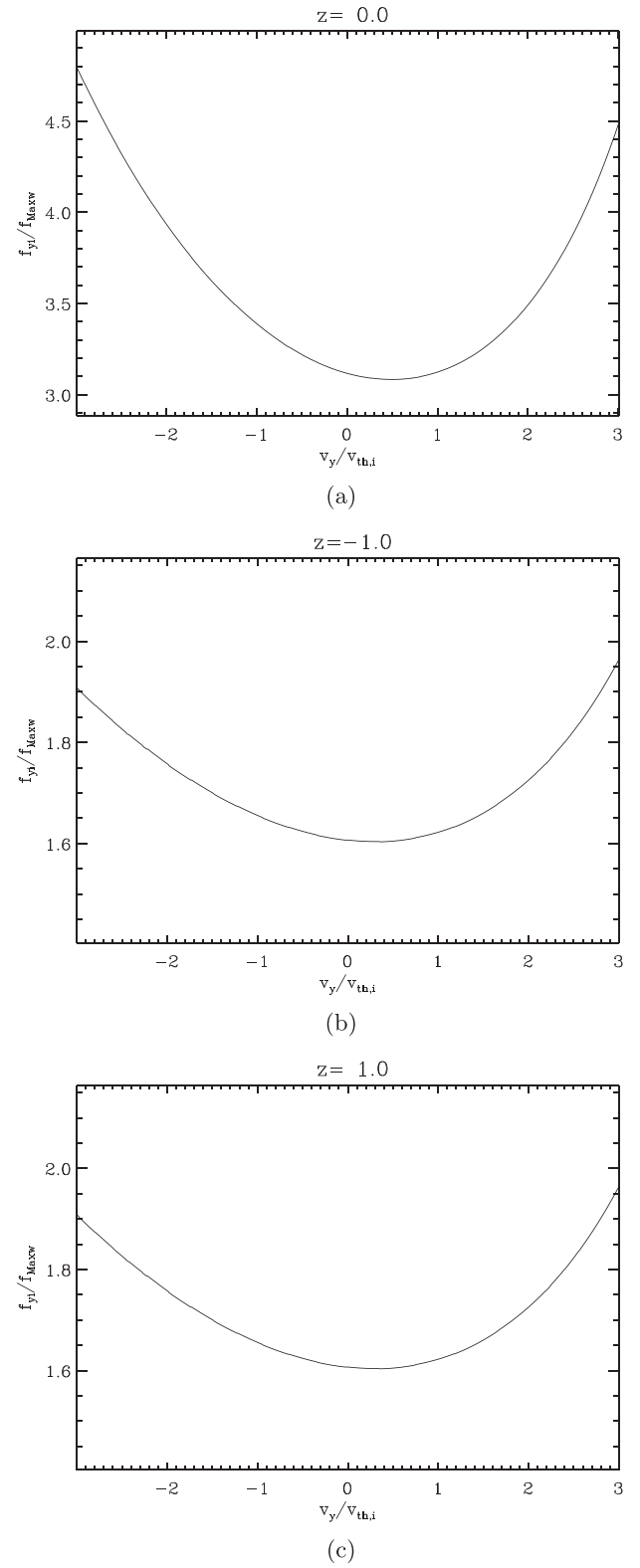
FIG. 2. The v_x variation of $f_i/f_{Maxw,i}$ for $z/L = 0$ (a), $z/L = -1$ (b), and $z/L = 1$ (c). $\beta_{pl} = 0.85$ and $\delta_i = 0.15$. Note the antisymmetry of the $z = \pm 1$ plots with respect to each other.

FIG. 3. The v_y variation of $f_i/f_{Maxw,i}$ for $z/L = 0$ (a), $z/L = -1$ (b), and $z/L = 1$ (c). $\beta_{pl} = 0.85$ and $\delta_i = 0.15$. Note the symmetry of the $z = \pm 1$ plots with respect to each other.

recurrence relation for the Hermite Polynomials. We acknowledge that this β_{pl} is only modestly below unity, however, it represents a value of which we are confident of our numerics for both the p_x and p_y dependent sums. In Figures 1(a)–1(c), we plot the v_x variation of our electron distribution function, as a representative example (the v_y plots are

qualitatively similar). First of all, we note that the DFs appear to have only a single maximum, and fall off as $v_x \to \pm\infty$. This is to be contrasted with the plots of the DF using the additive pressure,[25] which can have multiple peaks. Thus far we have not found any indication of multiple peaks in the parameter regime that we have been able to explore.
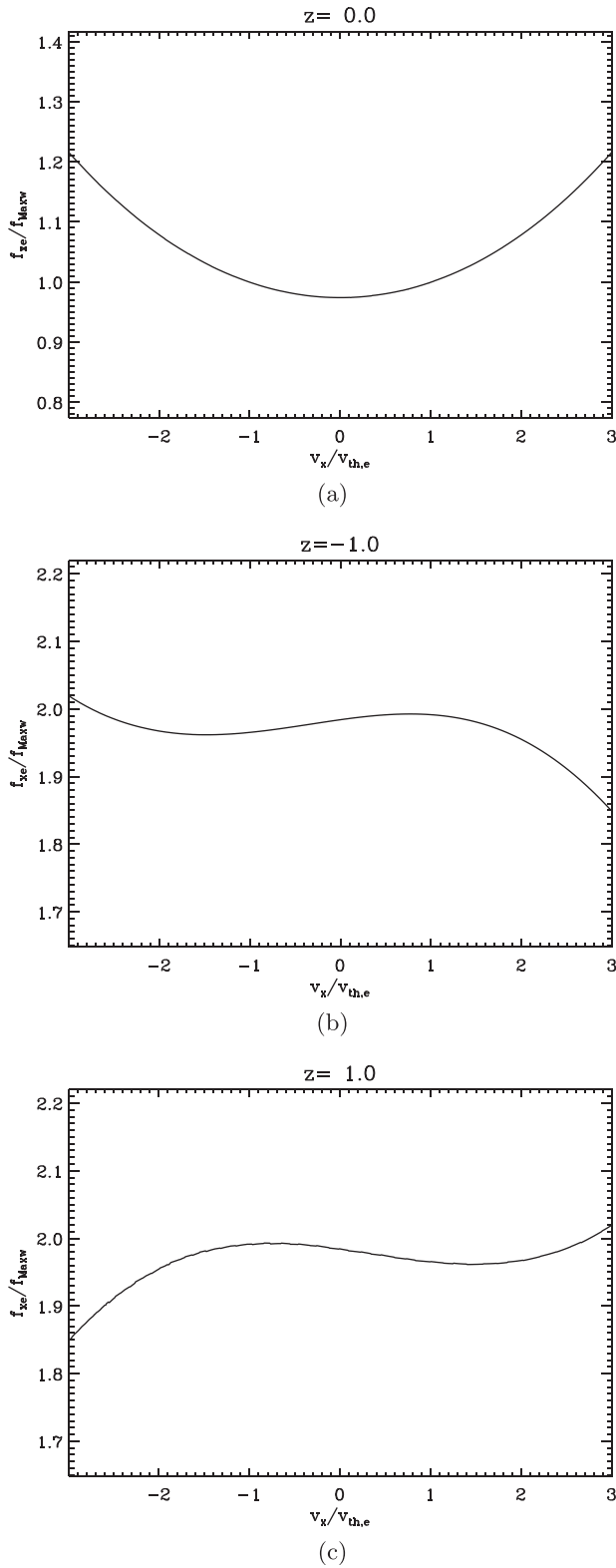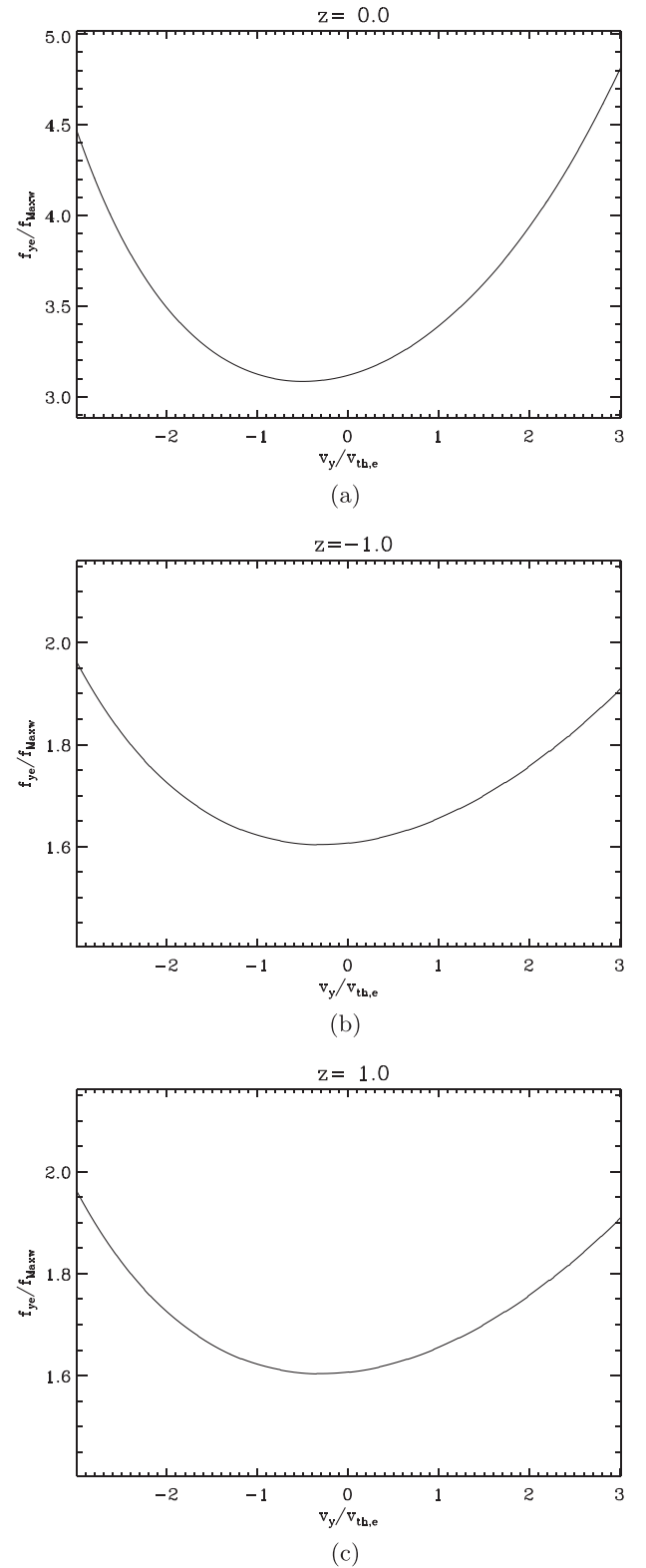
FIG. 4. The v_x variation of $f_e/f_{Maxw,e}$ for $z/L = 0$ (a), $z/L = -1$(b), and $z/L = 1$ (c). $\beta_{pl} = 0.85$ and $\delta_e = 0.15$. Note the antisymmetry of the $z = \pm 1$ plots with respect to each other.

FIG. 5. The v_y variation of $f_e/f_{Maxw,e}$ for $z/L = 0$ (a), $z/L = -1$ (b), and $z/L = 1$ (c). $\beta_{pl} = 0.85$ and $\delta_e = 0.15$. Note the symmetry of the $z = \pm 1$ plots with respect to each other.

However, this does not mean that multiple peaks cannot appear, for example, for lower values of the β_{pl}.

A first look at the plots also seems to indicate that the shape of the DF resembles the shape of a Maxwellian. Motivated by this similarity, we define a Maxwellian DF by

$$f_{Maxw,s} = \frac{n_0}{\left(\sqrt{2\pi} v_{th,s}\right)^3} \exp\left[\frac{\left(\mathbf{v} - \langle \mathbf{v} \rangle_s(z)\right)^2}{2v_{th,s}^2}\right]. \qquad (30)$$

The Maxwellian distribution reproduces the same first order moment in terms of z as the equilibrium solution does,
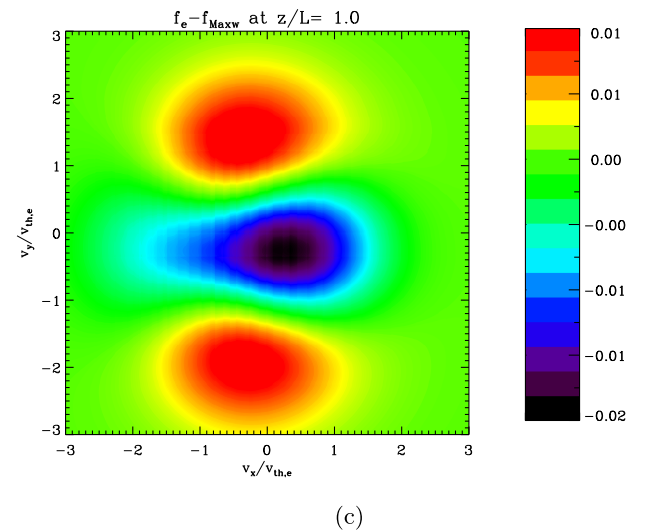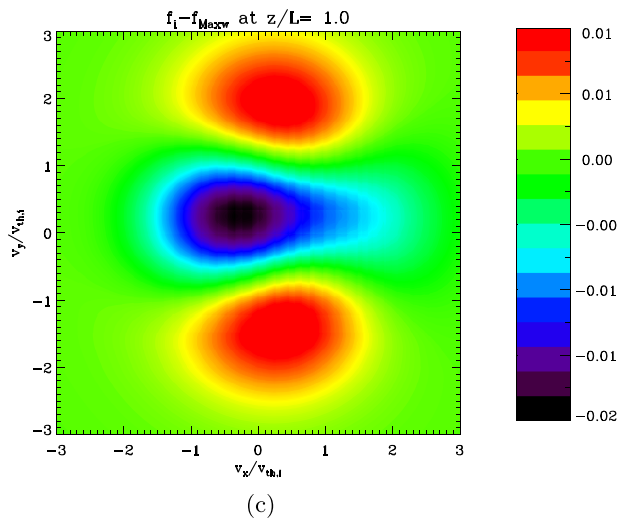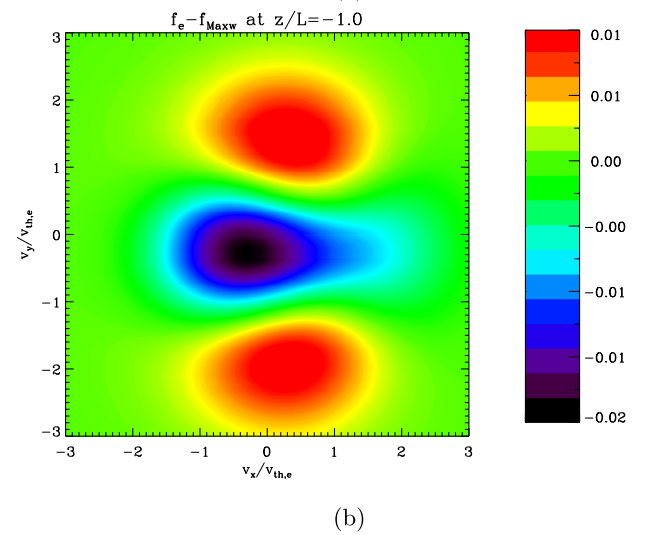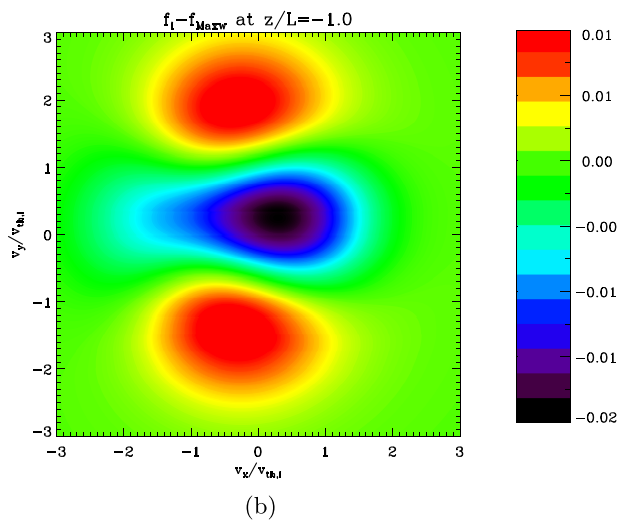
FIG. 6. Contour plots of $f_i - f_{Maxw,i}$ for $z/L = 0$ (a), $z/L = -1$ (b), and $z/L = 1$ (c). $\beta_{pl} = 0.85$ and $\delta_i = 0.15$. Note the antisymmetry of the $z = \pm 1$ plots with respect to each other.
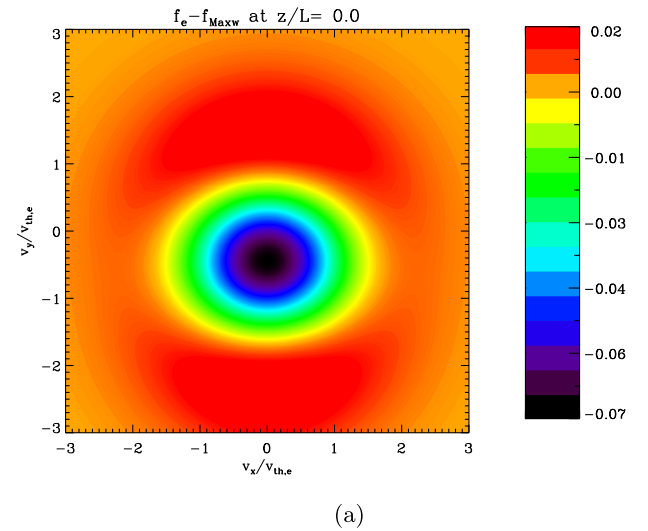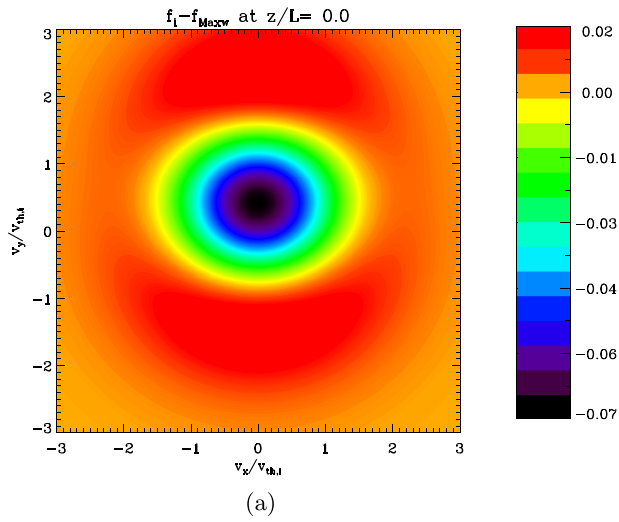
FIG. 7. Contour plots of $f_e - f_{Maxw,e}$ for $z/L = 0$ (a), $z/L = -1$ (b), and $z/L = 1$ (c). $\beta_{pl} = 0.85$ and $\delta_e = 0.15$. Note the antisymmetry of the $z = \pm 1$ plots with respect to each other.

namely, $n_0 \langle \mathbf{v} \rangle_s$, and a spatially uniform number density, namely, n_0. However, it is not a solution of the Vlasov equation and hence not an equilibrium solution. See Ref. 36 for an example of Particle in Cell simulations with a force-free field, initiated with a distribution of this type. To

highlight the difference between the two distribution functions, we plot the both the v_x and v_y variation of the ratio of the DF, with the Maxwellian of Equation (30) for both ions and electrons in Figures 2(a)–5(c). As we can see, in all plots the ratio deviates from unity, and in some cases these

deviations are substantial. This shows that the initial impression is somewhat misleading. We also observe a symmetry in that the v_y dependent plots are even in z, since A_y and $\langle v_y \rangle_s$ are even in z.

To further see the deviations of f_s from the Maxwellian, we present contour plots of the difference $f_s - f_{Maxw,s}$ in Figures 6(a)–7(c) over (v_x, v_y) space for various z values. One observation we can make from these is that there is a certain symmetry with respect to both velocity direction and the value of z. For example, it seems that f_s is symmetric under the transformation $(v_x \rightarrow -v_x, z \rightarrow -z)$. This seems reasonable since A_x is dynamically equivalent to an odd function of z, by a gauge transformation, as B_y is even. For a plasma-beta modestly below unity, and thermal Larmor radius roughly 15% of the current sheet width, we find distributions that are roughly Maxwellian in shape, but "shallower" at the centre of the sheet. At the outer edges of the sheet, this shallowness assumes a drop-shaped depression in the v_x direction, with localised differences for large v_y.

V. SUMMARY AND CONCLUSIONS

This paper contains a first analysis of a DF capable of describing low plasma beta, nonlinear force-free collisionless equilibria. In this paper, the emphasis has been on a discussion of properties of the DF. By using expressions for the moments of the DFs, we have derived the relationships between the micro- and macroscopic parameters of the equilibrium, in particular, the current sheet width. We have presented line-plots of the electron DF in the v_x direction as a representative example. These show that the DF has a single maximum in the v_x direction, and *seems* to resemble a Maxwellian, at least for the parameter range studied. However, a detailed comparison with a Maxwellian describing the same particle density and average velocity/current

density shows that there are significant deviations. This was corroborated by contour plots of the difference between the DF and the Maxwellian in the (v_x, v_y) plane.

While it has been shown[10] that the infinite series over Hermite polynomials are convergent for all parameter values, plotting the DF has been difficult for the low-beta regime, particularly the v_x dependent sum. Hence, further work on attaining numerical convergence for a wider parameter range is essential. It would be particularly interesting to find out whether the DF develops multiple peaks similar to the DF found for an additive form of P_{zz}.[25]

ACKNOWLEDGMENTS

APPENDIX A: THE v_x MOMENT

The first order moments of the DF are used to calculate the bulk velocity, and in turn the current density. It is useful to calculate the current density from the DF not only as a procedural check, but also to derive relations between the micro- and macroscopic parameters. We now take the first moment of the DF by v_x denoted by $[v_x f_s]$

$$
\begin{aligned}
[v_x f_s] &= \frac{1}{m_s^3} \int_{-\infty}^{\infty} \int_{-\infty}^{\infty} \int_{-\infty}^{\infty} v_x f_s d^3 p, \\
&= \frac{n_0 e^{-\frac{1}{2\beta_{pl}}}}{(\sqrt{2\pi}) m_s v_{th,s}} \sum_{n=0}^{\infty} b_n \left(\frac{A_y}{B_0 L} \right)^n \sum_{m=0}^{\infty} C_{2m,s} \underbrace{\int_{-\infty}^{\infty} v_x e^{-\frac{\beta_s}{2m_s}(p_{xs} - q_s A_x)^2} H_{2m} \left(\frac{p_{xs}}{\sqrt{2 m_s} v_{th,s}} \right) dp_{xs}}_{I_{v_x}},
\end{aligned}
$$

after both the p_{ys} and p_{zs} integrations. Now, use the Hermite expansion of the exponential,[37] to give

$$
I_{v_x} = \frac{1}{m_s} \int_{-\infty}^{\infty} (p_{xs} - q_s A_x) H_{2m} \left(\frac{p_{xs}}{\sqrt{2 m_s} v_{th,s}} \right) e^{-\frac{\beta_s p_{xs}^2}{2m_s}} \left[\sum_{j=0}^{\infty} \frac{1}{(j)!} \left(\frac{q_s A_x}{\sqrt{2 m_s} v_{th,s}} \right)^j H_j \left(\frac{p_{xs}}{\sqrt{2 m_s} v_{th,s}} \right) \right] dp_{xs}. \tag{A1}
$$

Define an inner product according to

$$
\langle f_1(x), f_2(x) \rangle = \int_{-\infty}^{\infty} e^{-x^2} f_1(x) f_2(x) dx. \tag{A2}
$$

Then orthogonality of the Hermite polynomials, $\langle H_k(x), H_l(x) \rangle = \sqrt{\pi} 2^k k! \delta_{kl}$, and the recurrence relation, $H_{n+1}(x) = 2x H_n(x) - 2n H_{n-1}(x)$, are used to give

$$\langle xH_j(x), H_{2m}(x)\rangle = j\langle H_{j-1}(x), H_{2m}(x)\rangle + \frac{1}{2}\langle H_{j+1}(x), H_{2m}(x)\rangle$$
$$= \sqrt{\pi} 2^{2m}(2m)! \left(j\delta_{j-1,2m} + \frac{1}{2}\delta_{j+1,2m} \right). \tag{A3}$$

This allows us to write

$$I_{v_x} = \sqrt{2\pi} v_{th,s} 2^{2m}(2m)! \sum_{j=0}^{\infty} \frac{1}{j!} \left(\frac{q_s A_x}{\sqrt{2} m_s v_{th,s}} \right)^j$$
$$\times \left[\sqrt{2} m_s v_{th,s} \left(j\delta_{j-1,2m} + \frac{1}{2}\delta_{j+1,2m} \right) - q_s A_x \delta_{j,2m} \right].$$

So we have

$$[v_x f_s] = \frac{n_0 e^{-\frac{1}{2\beta_{pl}}}}{m_s} \sum_{n=0}^{\infty} b_n \left(\frac{A_y}{B_0 L} \right)^n \sum_{m=0}^{\infty} C_{2m,s} 2^{2m}(2m)!$$
$$\times \sum_{j=0}^{\infty} \frac{1}{j!} \left(\frac{q_s A_x}{\sqrt{2} m_s v_{th,s}} \right)^j$$
$$\times \left[\sqrt{2} m_s v_{th,s} \left(j\delta_{j-1,2m} + \frac{1}{2}\delta_{j+1,2m} \right) - q_s A_x \delta_{j,2m} \right]$$

reducing to

$$[v_x f_s] = \left(\frac{m_s v_{th,s}^2}{q_s B_0 L} \right) n_0 e^{-\frac{1}{2\beta_{pl}}} \sum_{n=0}^{\infty} b_n \left(\frac{A_y}{B_0 L} \right)^n \sum_{m=1}^{\infty} a_{2m} 2m \left(\frac{A_x}{B_0 L} \right)^{2m-1}$$
$$= \left(\frac{m_s v_{th,s}^2}{q_s P_0} \right) n_0 \frac{\partial \bar{P}_{zz}}{\partial A_x} = \frac{\beta_e \beta_i}{\beta_e + \beta_i} \left(\frac{1}{q_s \beta_s} \right) \frac{\partial \bar{P}_{zz}}{\partial A_x}. \tag{A4}$$

The x component of current density is defined as $j_x = \sum_s q_s[v_x f_s]$, giving

$$j_x = \frac{\beta_e \beta_i}{\beta_e + \beta_i} \frac{\partial \bar{P}_{zz}}{\partial A_x} \sum_s \frac{1}{\beta_s} = \frac{\partial \bar{P}_{zz}}{\partial A_x}$$
$$\Rightarrow j_x = \frac{\partial \bar{P}_{zz}}{\partial A_x}, \tag{A5}$$

reproducing the familiar result.[5,12,18,24] The first moment of the DF can also be used to calculate the bulk velocity in terms of the microscopic parameters

$$\langle v_x \rangle_s = \frac{[v_x f_s]}{n_s} = \frac{j_x}{q_s \beta_s P_0}, \tag{A6}$$

using Equation (A4). Then, by using the current density for the FFHS,

$$\mathbf{j} = \frac{B_0}{\mu_0 L} \left(\frac{\sinh\left(\frac{z}{L}\right)}{\cosh^2\left(\frac{z}{L}\right)}, \frac{1}{\cosh^2\left(\frac{z}{L}\right)}, 0 \right), \tag{A7}$$

we have the fluid flow in x

$$\langle v_x \rangle_s = \frac{B_0}{\mu_0 L q_s \beta_s P_0} \frac{\sinh\left(\frac{z}{L}\right)}{\cosh^2\left(\frac{z}{L}\right)}. \tag{A8}$$

APPENDIX B: THE v_y MOMENT

By a completely analogous calculation, we derive the v_y moment of the DF

$$[v_y f_s] = \left(\frac{m_s v_{th,s}^2}{P_0 q_s} \right) n_0 \frac{\partial \bar{P}_{zz}}{\partial A_y} = \frac{\beta_e \beta_i}{\beta_e + \beta_i} \left(\frac{m_s v_{th,s}^2}{q_s} \right) \frac{\partial \bar{P}_{zz}}{\partial A_y}.$$

Again, the current density $j_y = \sum_s q_s[v_y f_s]$ gives

$$j_y = \frac{\beta_e \beta_i}{\beta_e + \beta_i} \frac{\partial P_{zz}}{\partial A_y} \sum_s m_s v_{th,s}^2 = \frac{\partial \bar{P}_{zz}}{\partial A_y}$$
$$\Rightarrow j_y = \frac{\partial \bar{P}_{zz}}{\partial A_y}.$$

We can also calculate the bulk velocity in terms of the microscopic parameters

$$\langle v_y \rangle_s = \frac{B_0}{\mu_0 L q_s \beta_s P_0} \frac{1}{\cosh^2\left(\frac{z}{L}\right)}. \tag{B1}$$

[1]T. Wiegelmann and T. Sakurai, Living Rev. Sol. Phys. **9**, 5 (2012).
[2]G. Marsh, *Force-Free Magnetic Fields: Solutions, Topology and Applications* (World Scientific, Singapore, 1996).
[3]R. Fitzpatrick, Phys. Plasmas **14**, 062505 (2007).
[4]T. Sakurai, Space Sci. Rev. **51**, 11 (1989).
[5]K. Schindler, *Physics of Space Plasma Activity* (Cambridge University Press, Cambridge, UK, 2007).
[6]E. Priest and T. Forbes, *Magnetic Reconnection* (Cambridge University Press, Cambridge, UK, 2000).
[7]M. G. Harrison and T. Neukirch, Phys. Rev. Lett. **102**, 135003 (2009).
[8]F. Wilson and T. Neukirch, Phys. Plasmas **18**, 082108 (2011).
[9]B. Abraham-Shrauner, Phys. Plasmas **20**, 102117 (2013).
[10]O. Allanson, T. Neukirch, S. Troscheit, and F. Wilson, "Particular solutions of the inverse problem for 1D Vlasov-Maxwell equilibria using Hermite polynomials," arXiv:1508.07925 [physics.plasm-ph].
[11]A. V. Artemyev, Phys. Plasmas **18**, 022104 (2011).
[12]P. J. Channell, Phys. Fluids **19**, 1541 (1976).
[13]A. Sestero, Phys. Fluids **10**, 193 (1967).
[14]N. A. Bobrova and S. I. Syrovatskiĭ, Sov. J. Exp. Theor. Phys. Lett. **30**, 535 (1979); available at http://www.jetpletters.ac.ru/ps/1368/article_20696.shtml.
[15]D. Correa-Restrepo and D. Pfirsch, Phys. Rev. E **47**, 545 (1993).
[16]N. A. Bobrova, S. V. Bulanov, J. I. Sakai, and D. Sugiyama, Phys. Plasmas **8**, 759 (2001).
[17]N. A. Bobrova, S. V. Bulanov, G. E. Vekstein, J.-I. Sakai, K. Machida, and T. Haruki, Plasma Phys. Rep. **29**, 449 (2003).
[18]M. G. Harrison and T. Neukirch, Phys. Plasmas **16**, 022106 (2009).
[19]H. Grad, Phys. Fluids **4**, 1366 (1961).
[20]B. Bertotti, Ann. Phys. **25**, 271 (1963).
[21]R. B. Nicholson, Phys. Fluids **6**, 1581 (1963).
[22]A. Sestero, Phys. Fluids **9**, 2006 (1966).
[23]N. Attico and F. Pegoraro, Phys. Plasmas **6**, 767 (1999).
[24]H. E. Mynick, W. M. Sharp, and A. N. Kaufman, Phys. Fluids **22**, 1478 (1979).
[25]T. Neukirch, F. Wilson, and M. G. Harrison, Phys. Plasmas **16**, 122102 (2009).
[26]D. V. Widder, Trans. Am. Math. Soc. **71**, 430 (1951).
[27]D. V. Widder, Bull. Am. Math. Soc. **60**, 444 (1954).
[28]G. G. Bilodeau, Duke Math. J. **29**, 293 (1962).
[29]G. B. Arfken and H. J. Weber, *Mathematical Methods for Physicists*, 5th ed. (Harcourt/Academic Press, Burlington, MA, 2001).

[30]E. T. Bell, Ann. of Math. **35**, 258 (1934).

[31]W. P. Johnson, Am. Math. Monthly **109**, 217 (2002).

[32]R. Fitzpatrick, *Plasma Physics: An Introduction* (CRC Press, Taylor & Francis Group, 2014).

[33]G. G. Howes, S. C. Cowley, W. Dorland, G. W. Hammett, E. Quataert, and A. A. Schekochihin, Astrophys. J. **651**, 590 (2006).

[34]D. W. Hewett, C. W. Nielson, and D. Winske, Phys. Fluids **19**, 443 (1976).

[35]A. Suzuki and T. Shigeyama, Phys. Plasmas **15**, 042107 (2008).

[36]M. Hesse, M. Kuznetsova, K. Schindler, and J. Birn, Phys. Plasmas **12**, 100704 (2005).

[37]P. M. Morse and H. Feshbach, *Methods of Theoretical Physics* (McGraw-Hill Book Co., 1953), Vol. 2.